Comprehensive study of ZnO films prepared by filtered cathodic vacuum arc at room temperature

Y. G. Wang, S. P. Lau,[a] H. W. Lee, S. F. Yu, and B. K. Tay
School of Electrical and Electronic Engineering, Nanyang Technological University, Singapore 639798, Singapore

X. H. Zhang
Institute of Materials Research and Engineering, Research Link, Singapore 117602, Singapore

K. Y. Tse and H. H. Hng
School of Materials Engineering, Nanyang Technological University, Singapore 639798, Singapore

(Received 13 February 2003; accepted 22 May 2003)

Room temperature deposition of high crystal quality zinc oxide (ZnO) films was realized by the filtered cathodic vacuum arc (FCVA) technique. Detrimental macroparticles in the plasma as byproducts of arcing process are removed with an off-plane double bend magnetic filter. The influence of oxygen pressure on the structural, electrical and optical properties of ZnO films were investigated in detail. The crystal structure of ZnO is hexagonal with highly *c*-axis orientation. Intrinsic stress decreases with an increase of chamber pressure, and near stress-free film was obtained at 1×10^{-3} Torr. Films with optical transmittance above 90% in the visible range and resistivity as low as $4.1\times10^{-3}\ \Omega$ cm were prepared at pressure of 5×10^{-4} Torr. Energetic zinc particles in the cathodic plasma and low substrate temperature enhance the probability of formation of zinc interstitials in the ZnO films. The observation of strong ultraviolet photoluminescence and weak deep level emission at room temperature manifest the high crystal quality of the ZnO films prepared by FCVA. Enlargement of the band gap is observed in the absorption and photoluminescence spectra, the band gap shifts towards lower energy with an increase of oxygen pressure. This phenomenon is attributed to the Burstein–Moss effect. © *2003 American Institute of Physics.* [DOI: 10.1063/1.1592007]

I. INTRODUCTION

Vacuum arc deposition is a well-established film preparation technique with increasing importance.[1–3] The cathodic arc plasma is characterized by a high ionization ratio and high ion drift energy. Various single element films including metals, silicon, and tetrahedral amorphous carbon have been deposited using this technique.[4–7] With the introduction of reactive gases into the system chamber and using a compound target, vacuum arc can be extended to deposit many ceramics coatings, semiconductor films and even high-temperature superconductor films.[1,3] Macrodroplets of 0.1–10 μm are unavoidable byproducts of the cathodic arc process, which can easily reach the substrate and cause contamination of the films.[2,8,9] This drawback hinders broad application of films using the cathodic vacuum arc in optical and electronic regimes, where uniformity and smoothness are prerequisites. Several attempts have been made to overcome this problem, among them use of curved magnetic ducts is most effective in filtering out macroparticles.[2,10,11] The plasma is guided through ducts by the magnetic field, and macroparticles moving along nearly straight trajectories are trapped at duct walls. The ions in the plasma obtain high energies of 10–200 eV at the cathode depending on the ion mass;[12] such high energy ions enhance the surface atom mobility, and in turn enable the deposition of dense high crystal quality films at relatively low substrate temperature.[1,13,14] Tetrahedral amorphous carbon,[7] polycrystalline *h*-AlN film[15] and rutile phase TiO_2 film[16] have been prepared by vacuum arc technique at room temperature.

ZnO is a multifunctional semiconductor material that has been used in various areas, including phosphors, piezoelectric transducers, surface acoustic wave devices, gas sensors and varistors.[17–21] With a band gap ($E_g=3.3$ eV) it is similar to that of GaN but with higher exciton binding energy (60 meV). ZnO is a promising material for short wavelength light emitting devices and daylight-blind UV detectors.[21,22] Since it is an important transparent conducting oxide, ZnO film has high transmittance in the visual region and low electrical resistivity with intrinsic defects or the dopant, and is an ideal window material for solar cell and flat panel displays.[23] ZnO films have been synthesized by numerous methods such as metalorganic chemical vapor deposition,[24,25] molecular beam epitaxy,[26] magnetron sputtering,[27–29] pulsed laser deposition,[30] atomic layer deposition,[31] spray pyrolysis,[32] and so on. Low temperature deposition is preferred in some processes in order to avoid reactive and elemental diffusion of different layers and to protect substrates such as polymers. Among these methods, ZnO films can be synthesized at temperature as low as 100 °C by metalorganic chemical vapor deposition and atomic layer deposition,[24,31] and even at room temperature by magnetron sputtering and pulsed laser

[a]Electronic mail: esplau@ntu.edu.sg

Downloaded 07 Aug 2003 to 155.69.4.4. Redistribution subject to AIP license or copyright, see http://ojps.aip.org/japo/japcr.jsp

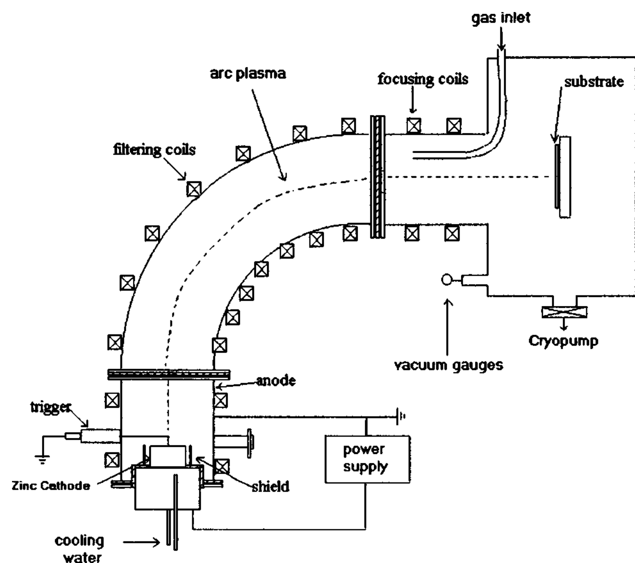

FIG. 1. Schematic diagram of the filtered cathodic vacuum arc deposition system.

deposition.[28,30] The high kinetic energies of growing precursors in the last two methods are believed to play a key role in the realization of low temperature deposition. By comparison, the filtered cathodic vacuum arc (FCVA), another energetic deposition technique, has received little attention for the preparation of ZnO films. Naoe and Nakagawa prepared ZnO films at temperature $\sim$600 °C by vacuum arc without macroparticle filtering.[33] Takikawa *et al.* deposited *c*-axis oriented ZnO films by a simple shielded vacuum arc without external heating in the pressure range of 1×10^{-3}–4×10^{-2} Torr, where the distance between the cathode and substrate was 20 cm.[34] Recently a FCVA equipped with an off-plane double bend (OPDB) filter, by which macrodroplet-free amorphous carbon films can be synthesized, was employed to prepare ZnO films.[35,36] The behavior of the FCVA with a long filter duct is distinct from other vacuum arcs in that it has background gas pressure dependence, an ion energy distribution and ion transport efficiency.[37] In this article, the feasibility of room temperature deposition of ZnO films by the FCVA is demonstrated, and the influence of the oxygen pressure on the structural, optical and electrical properties is investigated systematically.

II. EXPERIMENTS

A schematic diagram of the vacuum arc apparatus used in this study is shown in Fig. 1. The cathode is a 60 mm diam 99.99% purity zinc target mounted onto a water-cooled copper plate. The arc is ignited by a contact method using a retractable carbon striker. The arc was operated in dc mode with current of approximately 60 A. The anode was grounded to keep the plasma potential close to the ground. The OPDB filter was inserted between the plasma source and the main chamber, macroparticles produced in the cathodic arc plasma were removed effectively and the transport efficiency of this bend was similar to a commonly used single 90° filter bend. The magnetic filter consisted of three straight pieces and two tori; these two tori are actually 90° bends used cut to required angles of 65° and 45°, with the major radius R and minor radius r 135 and 50.8 mm, respectively. The bend was electrically isolated from the rest of the system. The toroidal magnetic field for steering the plasma beam through the filter was produced by copper coils wrapped around the bend and was kept at 40 mT during experiments.

The ZnO films were deposited on Si (001) and a glass substrate, which were mounted perpendicular to the direction of the plasma beam about 10 cm away from the outlet of the filter bend. The substrates were cleaned ultrasonically using acetone, methanol and ionized water consequently, and then blown dry with nitrogen gas. Oxygen (purity 99.99%) was used as the reactive gas; its flow rate was controlled by a mass flow meter kept at 60 sccm during deposition. The chamber was evacuated to a base pressure of 2×10^{-6} Torr before deposition. The working pressure was adjusted by varying the pumping rate. The chamber pressure decreases upon ignition of the arc, because oxygen gas is pumped by zinc plasma in a manner similar to that of a Ti sublimation pump; the pressure value used here was measured during the deposition process with arcing. The depositions were carried out at various pressures ranging from 10^{-4} to 10^{-3} Torr. The deposition time was adjusted to obtain films with thicknesses of about 200 nm. No external heating was used; however, the substrate temperature was increased slightly during deposition. The process temperature was measured to be below 45 °C by a thermocouple attached to the substrate surface.

The structural features of the ZnO films were studied by x-ray diffraction (XRD) (Shimadzu XRD-6000) in θ–2θ mode using Cu $K\alpha$ radiation. The film thickness was measured by a stylus surface profiler (Tencor P10). A field emission scanning electron microscope (SEM) and an atomic force microscope (AFM) (Nanoscope III, Digital Instruments) were used to characterize the surface morphology of the films. Optical transmittance measurements were performed with a double beam spectrometer in the wavelength range of 250–1050 nm. A photoluminescence (PL) spectrum was acquired in the wavelength range of 350–850 nm at room temperature; the excitation light was the 325 nm line of a He–Cd laser. The resistivity, carrier density and Hall mobility were measured at room temperature by the van der Pauw method.

III. RESULTS AND DISCUSSION

A. Structural properties

The main drawback that prevents wide application of the vacuum arc method for depositing optical and electronic films is the formation of macrodroplets in the arcing process. The off-plane double bend filter removes the droplet effectively and enables the preparation of clean films. The film surfaces were analyzed by optical microscopy and SEM, and no droplet was detected on the ZnO films. Figure 2 presents typical surface and cross-sectional SEM images of the film deposited under oxygen pressure of 6×10^{-4} Torr. The film displays a very smooth, uniform grain size and void-free surface. No droplet is observed, confirming the high filtering efficiency of the filter used here. From the cross-sectional

Downloaded 07 Aug 2003 to 155.69.4.4. Redistribution subject to AIP license or copyright, see http://ojps.aip.org/japo/japcr.jsp

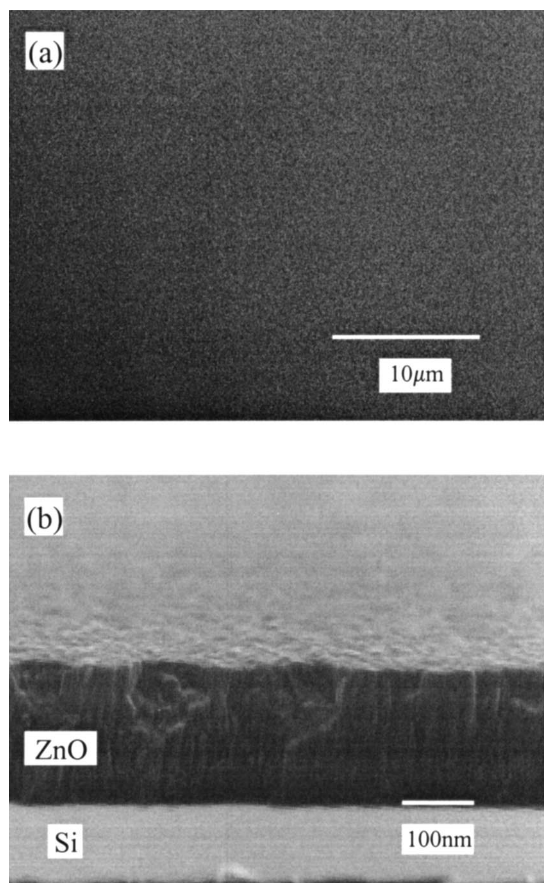

FIG. 2. SEM images showing the (a) surface and (b) cross-sectional morphology of ZnO film grown at oxygen pressure of 6×10^{-4} Torr.

image, it is seen that the film is composed of small column-like structures, which is consistent with the highly (001) texture growth evidenced by XRD analysis. Films deposited under different oxygen pressures were also evaluated by AFM. The AFM measurement was carried out in air, for each sample, and several locations with different scanning areas ranging from $0.5\times0.5\ \mu m^2$ to $10\times10\ \mu m^2$ were checked. Figure 3 shows typical images of films deposited at 2×10^{-4}, 5×10^{-4}, 8×10^{-4} and 1×10^{-3} Torr. The films are composed of well faceted grains, the sizes of which generally decrease with an increase of oxygen pressure. The root mean square (rms) roughness decreases from 3.9 [Fig. 3(a)] to 0.9 nm [Fig. 3(d)]. In the FCVA, the collision of zinc particles in the plasma with oxygen gas decreases the drift velocity and thus the kinetic energy.[37] The evolution of the grain size can be attributed to the variation of kinetic energy of the deposition atoms; at low oxygen pressure, the arriving particles have a higher kinetic energy, which enhances the diffusion of growth species on the film surface and favors the growth of larger grains.

Figure 4 shows $\theta/2\theta$ XRD spectra of the ZnO films deposited at different oxygen pressures. For oxygen pressure higher than 6.5×10^{-4} Torr, only the (002) diffraction peak at 34.4° appears in the spectra, which indicates the ZnO films are of hexagonal wurtzite crystal structure and with their *c* axis perpendicular to the substrate surface. At low oxygen pressure, the diffraction intensities are very low and diffraction peaks corresponding to (100) and (110) directions are observed at around 31.5° and 56.4°. The grains in the films are randomly oriented; no diffraction peak of the metallic zinc crystallite structure is detected. With a further decrease of the oxygen pressure, the films become opaque and display a metallic color, and peaks of zinc are detected (not shown). The diffraction intensity of the (002) direction increases with the oxygen pressure up to an optimum pressure of 8×10^{-4} Torr, and then decreases at higher pressures. This behavior can be understood by two competing processes; the increase of oxygen pressure in the chamber improves the stoichiometry of the films and the crystal quality. On the other hand, the kinetic energy of the reactive particles in the cathodic plasma decreases due to high oxygen pressure, which limits surface diffusion of the growing atoms and thus degrades the film quality.

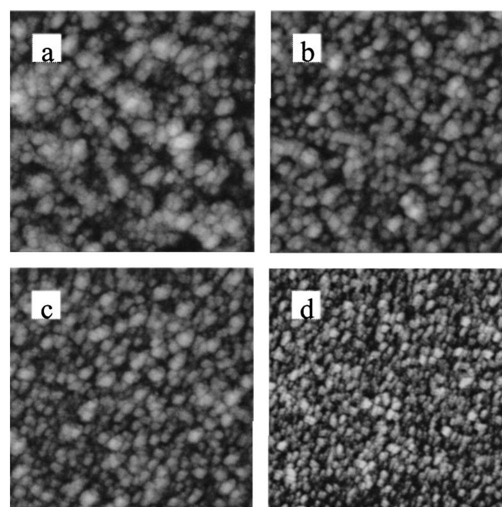

FIG. 3. AFM images of ZnO films deposited at oxygen pressures of (a) 2×10^{-4}, (b) 5×10^{-4}, (c) 8×10^{-4} and (d) 1×10^{-3} Torr. The dimensions are $1\times1\ \mu m^2$.

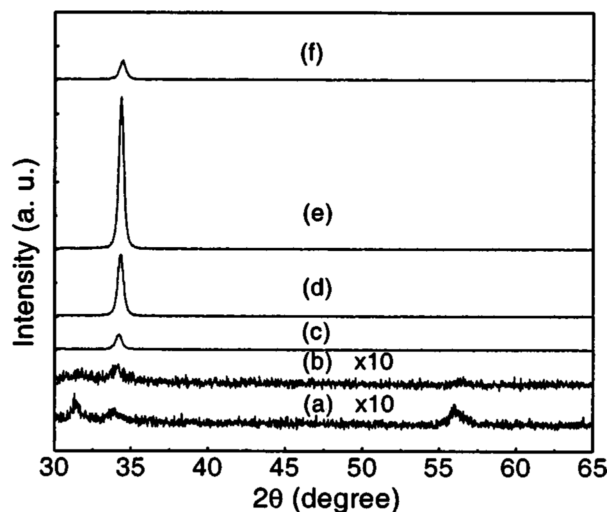

FIG. 4. XRD spectra of ZnO films prepared at oxygen pressures of (a) 2×10^{-4}, (b) 3.5×10^{-4}, (c) 5×10^{-4}, (d) 6.5×10^{-4}, (e) 8×10^{-4}, and (f) 1×10^{-3} Torr. Curves (a) and (b) are enlarged 10×.

Downloaded 07 Aug 2003 to 155.69.4.4. Redistribution subject to AIP license or copyright, see http://ojps.aip.org/japo/japcr.jsp

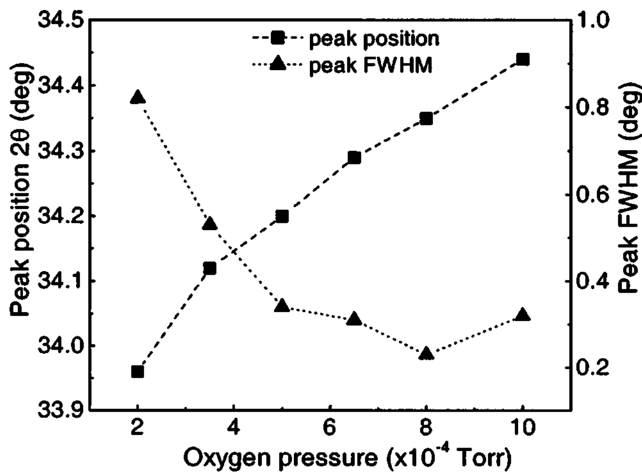

FIG. 5. Variation of the diffraction peak position and FWHM in the (002) direction with the oxygen pressure.

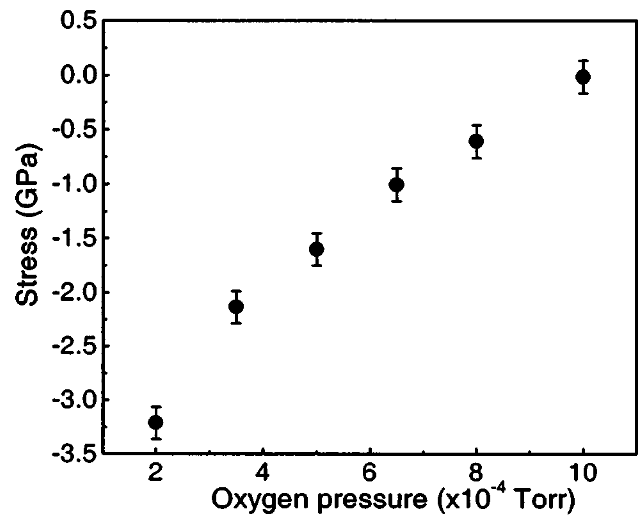

FIG. 6. Stress of the film estimated from the position of the (002) direction as a function of the oxygen pressure.

Figure 5 shows the full width at half maximum (FWHM) and position of the (002) diffraction peak as a function of the oxygen pressure. The FWHM was corrected for instrumental broadening using the (111) diffraction peak of the silicon monocrystal. It displays pressure dependence similar to the diffraction intensity; the smallest FWHM value of 0.23° is from the film grown at 8×10^{-4} Torr. The FWHM of XRD is influenced by many factors such as grain size, inhomogeneous stress distribution and crystal quality. From the AFM results, the grain size decreases with an increase of the oxygen pressure. This indicates that the observed changes of the FWHM with oxygen pressure cannot be explained by the grain size. It is well known that the nonuniform stress distribution will induce FWHM broadening; the films deposited at low pressure have higher stress as discussed later, and a large FWHM can be expected. Another possible reason is due to defects and imperfections in the grains; at low oxygen pressure the oxygen deficiency is more serious and more defects are present in the grains. Thus, this widens the diffraction peak. Compared with standard data of the (002) peak, it is obvious that the peak position shifts towards low value, which manifests itself by the existence of compressive stress in the films, especially in the films deposited at low oxygen pressure. The stress in highly texturized films can be calculated based on the biaxial strain model using interlayer spacing of the films. The stress in the plane of ZnO film with a hexagonal crystal structure can be expressed as[38]

$$\sigma=\frac{2c_{13}^2-c_{33}(c_{11}+c_{12})}{2c_{13}}\,\frac{c-c_0}{c_0}. \tag{1}$$

The values of the elastic constant from single crystalline ZnO are used, $C_{11}=208.8$ GPa, $C_{33}=213.8$ GPa, $C_{12}=119.7$ GPa and $C_{13}=104.2$ GPa. C_0 is the interlayer spacing of the c axis. Substituting these values in the above equation gives $\sigma=-233(c-c_0/c_0)$ GPa. Figure 6 shows stress versus the deposition pressure; the error bar shows the uncertainty of the lattice parameters of the ZnO and experimental errors. The stress is compressive and varies from 3.2 GPa to nearly free of stress when the oxygen pressure increases from 2×10^{-4} to 1×10^{-3} Torr. The substrate temperature stays below 45 °C during deposition; the thermal stress due to various linear thermal expansion coefficients of the substrate and the ZnO film is negligible compared to the stress measured. The variation of stress in the film with the pressure by the FCVA is similar to that by the sputtering method.[28,38] In general, energetic bombardment of the growing film leads to compressive stress because of atomic peening, an energy dependent process. High oxygen pressure causes thermalization of the energetic species and so decreases the kinetic energy of the species that induces atomic peening. In the FCVA, this loss of energy is significant, due to the fact that the distance from the target surface to the substrate is about 1 m which is much longer than the distance between the target and substrate in sputtering and laser deposition systems. The films display no tensile stress in the pressure range studied. In sputtered ZnO films, no tensile stress was detected over a wide range of pressure either, and this was attributed to additional oxygen incorporated into the films.[39] On the other hand, from analysis of the energy of the species it is indicated that even at high pressure, there still exists a small percentage of high energy ions in the plasma which can induce slight compressive stress in the film.[37] That is why no tensile stress is present in the films.

The deposition rate of the ZnO films as a function of the oxygen pressure is shown in Fig. 7. The deposition rate was estimated from the film thickness and the corresponding deposition time. The growth rate decreases with an increase of the oxygen pressure. The transport efficiency of the filter bend decreases with an increase of the chamber pressure because of an increase in collision frequency of ions with gas atoms. The brightness of the plasma weakens with an increase in pressure. When the pressure reaches 2×10^{-3} Torr, no film can be deposited.

B. Electrical properties

Figure 8 shows variations of the resistivity, Hall mobility and carrier concentration of the ZnO films with respect to the oxygen pressure. All the films are in n-type conduction; their

Downloaded 07 Aug 2003 to 155.69.4.4. Redistribution subject to AIP license or copyright, see http://ojps.aip.org/japo/japcr.jsp

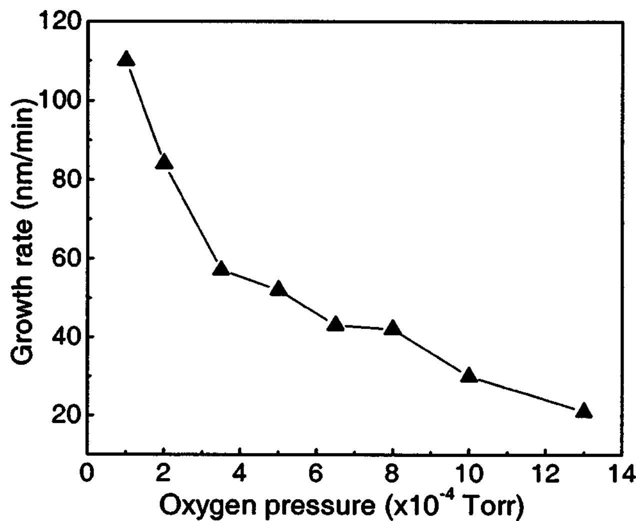

FIG. 7. Dependence of the growth rate of the ZnO films on the oxygen pressure.

resistivities first decrease with an increase of the oxygen pressure and reach a minimum resistivity of $4.1 \times 10^{-3}\ \Omega$ cm at pressure of about 5×10^{-4} Torr and then increase. The electrons in undoped ZnO films are normally attributed to intrinsic donors, but oxygen vacancies and zinc interstitials have frequently been invoked as the source of electrons.[17,40] From Fig. 8, we see the carrier concentration decreases with an increase of the oxygen pressure. The oxygen vacancy was originally considered responsible for the observed n-type conduction in ZnO.[40] Recently more experimental and theoretical work has found that the zinc interstitial is the main cause of electrons in undoped ZnO. Electron irradiation experiments by Look *et al.* showed that the zinc interstitial is most likely the cause of a shallow donor in ZnO.[41] Theoretical calculations indicate that the zinc interstitial is a shallow donor, and that the oxygen vacancy is a deep donor about 0.6 or 0.7 eV from the conduction band.[42,43] Hydrogen acts as a shallow donor and is suggested to be responsible for n-type conduction in nominally undoped ZnO films.[44–46] However, in our case, the hydrogen concentration in the film should be very trivial if it even exists. If the background hydrogen partial pressure in the reactive chamber is large enough and it acts as a determining factor in the electrical properties of the films, we would not expect the carrier concentrations of the films to display such regular strong oxygen pressure dependence behavior. For the same reason, the effects of other impurities, such as aluminum, can also be excluded, so the zinc interstitial should be the most likely to explain the observed high carrier concentrations. Hall mobility reflects the scattering processes of carriers in the films. In an undoped polycrystalline film, carriers are scattered mainly by intrinsic defects and grain boundaries, and other mechanisms such as lattice vibration scattering can be neglected. The grain boundary scattering depends on the grain size and electron mean free path in the films. The mean free path of electrons in the films can be roughly estimated by the highly degenerate electron model using the formula,[47]

$$l=\left(\frac{h}{2e}\right)\left(\frac{3n}{\pi}\right)^{1/3}\mu, \tag{2}$$

where n is the carrier concentration and μ is the Hall mobility. Using the data in Fig. 8, the mean free path of the electron is estimated to be below 2 nm. The grain sizes are about tens of nanometers as characterized by AFM, so intragrain scattering is dominant. The defects within the grains cause the observed low Hall mobility. The Hall mobility increases gradually with the pressure up to 8×10^{-4} Torr, and it decreases slightly with a further increase in pressure. The mobility values are lower than those of the films deposited at high temperature, but are similar to the films deposited at room temperature by other methods.[27,29] The ZnO films are stable in air after storage for several months. Their conductivities remain unchanged. Annealing experiments indicate that the films can withstand temperatures up to 200 °C in air without changing their electrical and optical properties.

C. Optical properties

Transmittance spectra in the ultraviolet and visible ranges of ZnO films grown under different oxygen pressures on a quartz substrate are shown in Fig. 9. It is seen that the transmittance of the films improves with an increase of the oxygen pressure. A steep falloff is observed at around 380 nm in the films deposited at oxygen pressure above 3.5×10^{-4} Torr, which is characteristic of high crystal quality ZnO films. The oscillations in the spectra are caused by optical interference on the smooth surface. The average transmittance in the visible region of the films deposited at 1×10^{-4} and 2×10^{-4} Torr is 30% and 50%, respectively. The two spectra are similar to those of amorphous material and no sharp absorption edge appears in them. This confirms again that the crystal quality deteriorates for strong oxygen deficiency conditions at low gas pressure. For the films deposited at pressure higher than 3.5×10^{-4} Torr, the average transmittance is above 90%. By applying the Tauc model,[48] the band gap of the films with steep falloff can be deduced from a plot of the square of absorption coefficient α^2 versus photon energy $h\nu$, and extrapolating the straight line portion of this plot to the energy axis. The optical band gaps of the samples prepared at pressures of 3.5×10^{-4}, 5×10^{-4}, 6.5

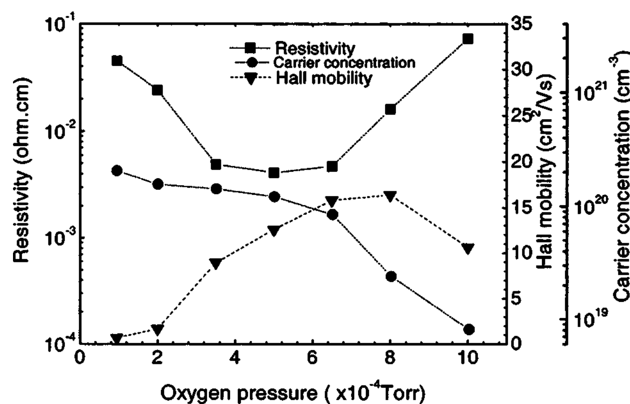

FIG. 8. Carrier concentration, Hall mobility and resistivity of ZnO films as a function of the oxygen pressure.

Downloaded 07 Aug 2003 to 155.69.4.4. Redistribution subject to AIP license or copyright, see http://ojps.aip.org/japo/japcr.jsp

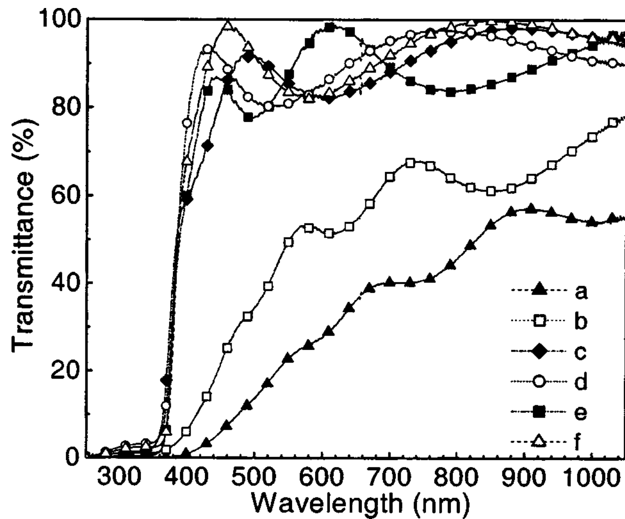

FIG. 9. Optical transmittance of ZnO films prepared at different oxygen pressures: (a) 1×10^{-4}, (b) 2×10^{-4}, (c) 3.5×10^{-4}, (d) 5×10^{-4}, (e) 6.5 $\times10^{-4}$, and (f) 8×10^{-4} Torr.

$\times10^{-4}$ and 8×10^{-4} Torr are 3.32, 3.31, 3.28 and 3.27 eV, respectively. The variation in band gap with the oxygen pressure has the same tendency as the carrier concentration, and the film with higher carrier concentration displays a larger band gap. This phenomenon, known as the Burstein–Moss effect, is induced by the blocking of low energy transitions in the conduction band of a degenerate semiconductor with free electrons, and it has been reported in ZnO films.[29,49]

PL spectra were acquired at room temperature. Luminescent peaks are observed in the films deposited at oxygen pressures of 3.5×10^{-4}, 5×10^{-4}, 6.5×10^{-4} and 8 $\times10^{-4}$ Torr, as shown in Fig. 10(a). No signal can be observed from the films grown under other conditions. Similar to the reported PL spectrum of ZnO deposited as high temperature, the spectra are composed of two parts, an excitonic related near band edge (NBE) emission peak in the ultraviolet region and a broad deep level emission band at around 610 nm (2.03 eV).[26] At room temperature, the NBE is dominated by free excitonic recombination. The origin of the deep level emission band is still not well understood and has been ascribed to oxygen vacancies, oxygen interstitials and Cu impurities.[18,50,51] The intensity of this band increases with an increase of the oxygen pressure. The appearance of NBE emission in the room temperature spectra and the high intensity ratio of NBE to deep level emission show the ZnO films are of high crystal quality. The high electron concentrations in our films may also improve ultraviolet excitonic luminescence by passivating deep level emission related defect centers and nonradiative centers. This kind of passivation effect has been found in ZnO with high carrier concentration and in hydrogen doped ZnO.[51,52] The variation of NBE with the oxygen pressure shows a trend similar to that in the XRD data; it first increases and then decreases. However, in comparing the PL spectra with XRD in Fig. 4, it can be seen that the NBE emission is not very consistent with the film quality evaluated from the XRD spectra. The strongest XRD peak appears in the film deposited at pressure of 8×10^{-4} Torr, whereas the highest NBE emission is achieved with oxygen

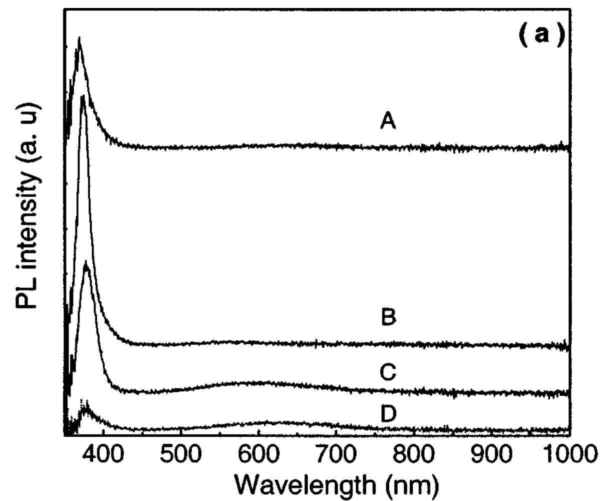

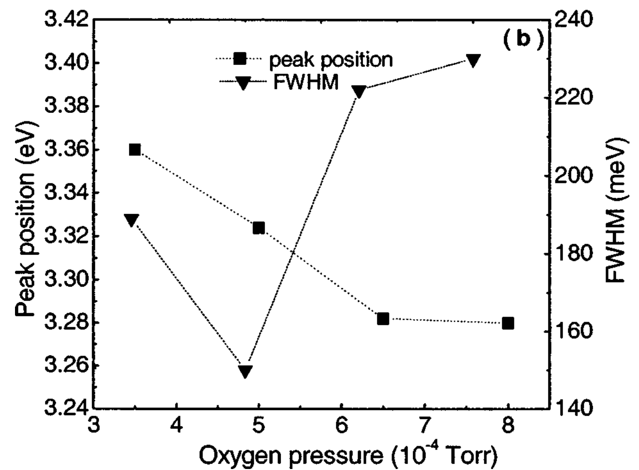

FIG. 10. (a) Room temperature PL spectra of ZnO films grown at various oxygen pressures: (A) 3.5×10^{-4}, (B) 5×10^{-4}, (C) 6.5×10^{-4}, and (D) 8 $\times10^{-4}$ Torr. (b) PL peak position and FWHM vs the oxygen pressure.

pressure of 5×10^{-4} Torr. A similar discrepancy between PL and XRD was also reported by Im *et al.* in pulsed laser deposited ZnO films.[53] It possibly originates from the fact that the sensitivity of PL and XRD is different for different kinds of defects. The excitonic Bohr radius of ZnO is 1.8 nm, and it is more sensitive to the density of point defects; XRD is more sensitive to imperfections of relatively large scale, such as dislocations, grain boundaries and mutual orientation of grains in the film. Another possible contribution to this phenomenon is different carrier concentrations; the carrier concentration in the film deposited at 5×10^{-4} Torr is 1.2 $\times10^{20}$ cm^{-3}, higher than that of 2.4×10^{19} cm^{-3} in the film prepared at 8×10^{-4} Torr; more nonradiative recombination centers and deep level emission centers are passivated in the former film than in the latter.

Figure 10(b) shows the FWHM and position of the NBE emission. The FWHM has its lowest value of 150 meV in the film deposited at pressure of 5×10^{-4} Torr. The peak positions shift towards lower energies with an increase of the oxygen pressure; this trend is consistent with the variation in band gap estimated from the absorption data. The energy of the NBE peak from free exciton recombination is normally lower than that of the band gap of the corresponding film,

Downloaded 07 Aug 2003 to 155.69.4.4. Redistribution subject to AIP license or copyright, see http://ojps.aip.org/japo/japcr.jsp

because of the exciton binding energy (~60 meV for ZnO) and Stokes shift. However, as can be seen, the NBE peak position is already higher than the corresponding band gap deduced from the absorption data. Srikant and Clarke compared the band gap of ZnO from different methods, and found that the band gap derived from optical absorption was lower than that from other methods and attributed it to a valence band–donor transition.[54] The dispute between the NBE peak position and the band gap may be due to the same reason.

D. Discussion

From the results, we can see that uniform high quality ZnO films can be synthesized by the FCVA method at room temperature. The film properties depend strongly on the oxygen pressure. Vacuum arc deposition is an energetic deposition process; metal ions obtain high drift energy in the range of 10–200 eV depending on the source material at the cathode. For the zinc ion, the drift kinetic energy E_{drift} obtained is ~36 eV according to Ref. 13. In our experiment, the substrate is in a floating condition, where sheath voltage V_{sheath} measured to be around 10 eV forms between the substrate and the plasma. Ionized zinc particles that arrive at the growth surface acquire total kinetic energy, $E_t = E_{\mathrm{drift}} + eQ_i V_{\mathrm{sheath}}$, and for single ions the value is ~46 eV; this high energy provides a kind of pseudotemperature for the film and improves the mobility of surface adatoms, which in turn favors the synthesis of crystalline films and eliminates the need for substrate heating that is normally indispensable in other methods, such as spray pyrolysis, molecular beam epitaty (MBE) and metalorganic chemical vapor deposition (MOCVD). For synthesis of ZnO film, suitable oxygen pressure is another important parameter as discussed earlier. The plasma properties in the FCVA are greatly influenced by background gases, and as of now only a few investigations have been carried out on this subject. Bilek *et al.* studied the effects of oxygen and nitrogen gases on the ion energy distributions of ionized species of carbon, titanium and aluminum filtered cathodic vacuum arcs; a reduction of 10 eV was reported for carbon arc plasma when the residual nitrogen pressure was increased from 1×10^{-5} to 1×10^{-3} Torr.[10,55] Lepone and co-workers investigated the interaction of copper cathodic plasma and oxygen background gases.[56,57] The specifics of the interactions are different for different metals and gases, however the main process that takes place should be similar. Generally the variations that take place upon the introduction of oxygen gas into a reactive chamber can be summarized as follows: (1) the mean kinetic energy of the zinc ions decreases through collision with oxygen gas; (2) the total ion current is reduced as the background gas pressure is increased, while the neutral zinc intensity increases; (3) formation of oxygen ions such as O_2^+ through energetic charge exchange collisions of zinc ions with oxygen molecules, chemical bonding like Zn–O may also be produced but in small density. High energy species are essential for the preparation of high quality ZnO films at low temperature, but to date, near room temperature deposition is only realized by energetic deposition methods, such as sputtering and pulsed laser techniques. From the above analysis, oxygen gas decreases the kinetic energy of the Zn ion directly through collision and the conversion of Zn ions to neutrals. Neutrals cannot obtain kinetic energy from the sheath region. The oxygen ions and Zn–O bonds can improve the film quality, however their relative densities are very small, so they contribute very little to the film quality. Recently, Anders pointed out that, in the FCVA process, the potential energy of metal ions should also be considered.[13] The potential energies of Zn^+ and Zn^{2+} are 9.39 and 27.4 eV, respectively, which in fact are comparable to the kinetic energy. The release mechanism of potential energy is not clear,[13] which prevents us from evaluating the portion of potential energy that contributes to film growth. The total potential energies are determined by the ion density and its charge state, so the potential energy should obey the same oxygen pressure dependence as the kinetic energy, i.e., a decrease in potential energy with an increase of oxygen pressure. From the above analysis, we can see that film quality is determined by two parameters, oxygen pressure and average species energy. They behave in opposite ways: as the oxygen pressure increases the stoichiometry of the ZnO films improves; however at the same time the energies of growing species, which are critical for the realization of low temperature growth, decreases. The interaction of the two parameters results in the synthesis of high quality ZnO films in a certain pressure range, which turns out to be in the range of 3.5×10^{-4}–1.0×10^{-3} Torr.

The ZnO films prepared by the FCVA show relatively low resistivity compared with the value reported.[28] As discussed above, the possibility of unintentionally doped impurities can be excluded. Under the same experimental conditions, when the substrate temperature is elevated, the resistivity of the film increases several orders of magnitude. The resistivity can be as high as $1\times10^{6}\ \Omega\,\mathrm{cm}$ for the film deposited at substrate temperature of 250 °C and oxygen pressure of 9×10^{-4} Torr. This further proves that the high carrier concentration in the low temperature deposited films originates from intrinsic defects and zinc interstitials, but not from impurities. The zinc interstitial has high formation energies and low diffusion barriers,[43,58] and it is unlikely to be incorporated in stable fashion. This can explain why the resistivity of undoped ZnO films deposited at high temperature is normally very high. The resistivity of the film can remain unchanged only up to 200 °C, which is much lower than that of aluminum doped ZnO films. This confirms that the zinc interstitial is unstable and is easily diffused into the ZnO crystal lattice. The production of a high concentration of zinc interstitials in the films by the FCVA can be attributed to two factors: (1) the high energy of zinc ions and (2) the low substrate temperature, which push the growth conditions from equilibrium. High ion energy facilitates the implantation of the zinc atom into the interstitial position, and increases the formation probability of zinc interstitials. Low substrate temperature prevents the diffusion of zinc interstitials into the ZnO crystal lattice and stabilizes the zinc interstitials.

Downloaded 07 Aug 2003 to 155.69.4.4. Redistribution subject to AIP license or copyright, see http://ojps.aip.org/japo/japcr.jsp

IV. CONCLUSIONS

High transparency (>90%) low resistivity ($4.1\times10^{-3}\ \Omega$ cm) ZnO films were grown on silicon and quartz glass by FCVA at room temperature. Highly *c*-axis oriented films were prepared in the pressure range of 5×10^{-4}–1×10^{-3} Torr, and the optimal pressure was around 8×10^{-4} Torr. The high carrier concentration in the films is attributed to zinc interstitials. The high ion energy and low substrate temperature increase the formation probability of zinc interstitials. An intense ultraviolet PL peak is detected. The PL peak position shifts towards lower energy with an increase of the oxygen pressure, which is consistent with the band gap determined from the absorption spectra, and is attributed to Burstein–Moss effect. High energy ions improve the mobility of growth species on the film surface and lead to the deposition of ZnO films. With the increase of oxygen pressure, species energies decrease greatly, so at low temperature high quality films can be synthesized only in a narrow oxygen pressure range of 3.5×10^{-4}–1×10^{-3} Torr in the FCVA system.

ACKNOWLEDGMENTS

This work was supported by the Agency for Science, Technology and Research (A*STAR) of Singapore and the Nippon Sheet Glass Foundation for Materials Science and Engineering.

[1] I. G. Brown, Annu. Rev. Mater. Sci. **28**, 243 (1998).
[2] R. L. Boxman, IEEE Trans. Plasma Sci. **29**, 762 (2001).
[3] P. J. Martin and A. Bendavid, Thin Solid Films **394**, 1 (2001).
[4] S. Anders, A. Anders, and I. G. Brown, J. Appl. Phys. **74**, 4239 (1993).
[5] I. G. Brown, Rev. Sci. Instrum. **65**, 3061 (1994).
[6] M. M. M. Bilek and W. I. Milne, Electron. Lett. **32**, 2016 (1996).
[7] D. R. McKenzie, D. A. Muller, and B. A. Pailthorpe, Phys. Rev. Lett. **67**, 773 (1991).
[8] T. Utsumi and J. H. English, J. Appl. Phys. **46**, 126 (1974).
[9] D. T. Tuma, C. L. Chen, and D. K. Davies, J. Appl. Phys. **49**, 3821 (1978).
[10] M. M. M. Bilek, Y. B. Yin, and D. R. Mckenize, IEEE Trans. Plasma Sci. **34**, 1165 (1996).
[11] A. Anders and R. A. MacGill, Surf. Coat. Technol. **133/134**, 96 (2000).
[12] I. A. Krinberg and M. P. Lukovnikova, J. Phys. D **29**, 2901 (1996).
[13] A. Anders, Appl. Phys. Lett. **80**, 1100 (2002).
[14] O. R. Monterio, Annu. Rev. Mater. Sci. **31**, 111 (2001).
[15] D. Manova, P. Huber, S. Mandl, and B. Rauschenbach, Surf. Coat. Technol. **142–144**, 61 (2001).
[16] H. Takikawa, T. Matsui, T. Sakakibara, A. Bendavid, and P. Martin, Thin Solid Films **34**, 186 (1999).
[17] D. C. Look, Mater. Sci. Eng., B **80**, 383 (2001).
[18] K. Vanheusden, W. L. Warren, C. H. Seager, D. R. Tallant, J. A. Voight, and B. E. Gnade, J. Appl. Phys. **79**, 7983 (1996).
[19] N. Chubachi, Proc. IEEE **64**, 772 (1976).
[20] U. Lampe and J. Muller, Sens. Actuators **18**, 269 (1989).
[21] D. R. Clarke, J. Am. Ceram. Soc. **82**, 485 (1999).
[22] D. M. Bagnall, Y. F. Chen, Z. Zhu, T. Yao, S. Koyama, M. Y. Shen, and T. Goto, Appl. Phys. Lett. **70**, 2230 (1997).
[23] R. Scheer, T. Walter, H. W. Wshock, M. L. Fearheiley, and H. J. Lewerenz, Appl. Phys. Lett. **63**, 3294 (1993).
[24] S. J. Baik, J. H. Jang, C. H. Lee, W. Y. Cho, and K. S. Lim, Appl. Phys. Lett. **70**, 3516 (1997).
[25] S. Muthukumar, C. R. Gorla, N. W. Emanetoglu, S. Liang, and Y. Lu, J. Cryst. Growth **225**, 197 (2001).
[26] Y. Chen, D. M. Bagnall, H. J. Koh, K. T. Park, K. Hiraga, Z.-Q. Zhu, and T. Yao, J. Appl. Phys. **84**, 3912 (1998).
[27] Z. L. Pei, C. Sun, M. H. Tan, J. Q. Xiao, D. H. Guan, R. F. Huang, and L. S. Wen, J. Appl. Phys. **90**, 3432 (2001).
[28] R. Cebulla, R. Wendt, and K. Ellmer, J. Appl. Phys. **83**, 1087 (1998).
[29] K. H. Kim, K. C. Park, and D. Y. Ma, J. Appl. Phys. **81**, 7764 (1997).
[30] L. N. Dinh, M. A. Schildbach, M. Balooch, and W. McLean II, J. Appl. Phys. **86**, 1149 (1999).
[31] A. Yamada, B. S. Sang, and M. Konagai, Appl. Surf. Sci. **112**, 216 (1997).
[32] S. A. Studenikin, N. Golego, and M. Cocivera, J. Appl. Phys. **84**, 2287 (1998).
[33] M. Naoe and S. Nakagawa, IEEE Trans. Magn. **29**, 3096 (1993).
[34] H. Takikawa, K. Kimura, R. Miyano, and T. Sakakibara, Thin Solid Films **377/378**, 74 (2000).
[35] X. Shi, B. K. Tay, H. S. Tan, E. Liu, J. Shi, L. K. Cheah, and X. Jin, Thin Solid Films **345**, 1 (1999).
[36] X. L. Xu, S. P. Lau, J. S. Chen, G. Y. Chen, and B. K. Tay, J. Cryst. Growth **223**, 201 (2001).
[37] M. M. M. Bilek, P. J. Martin, and D. R. Mckenzie, J. Appl. Phys. **83**, 2965 (1998).
[38] S. Maniv, W. D. Westwood, and E. Colombini, J. Vac. Sci. Technol. **20**, 162 (1982).
[39] J. Hinze and K. Ellmer, J. Appl. Phys. **88**, 2443 (2000).
[40] F. A. Kroger, *The Chemistry of Imperfect Crystals* (North-Holland, Amsterdam, 1974).
[41] D. C. Look, J. W. Hemsky, and J. R. Sizelove, Phys. Rev. Lett. **82**, 2552 (1999); F. D. Auret, S. A. Goodman, M. J. Legodi, and W. E. Meyer, Appl. Phys. Lett. **80**, 1340 (2002).
[42] S. B. Zhang, S.-H. Wei, and A. Zunger, Phys. Rev. B **63**, 075205 (2001).
[43] F. Oba, S. R. Nishitani, S. Isotani, H. Adachi, and I. Tanaka, J. Appl. Phys. **90**, 824 (2001).
[44] C. G. Van de Walle, Phys. Rev. Lett. **85**, 1012 (2000).
[45] D. M. Hofmann, A. Hofstaetter, F. Leiter, H. Zhou, F. Henecher, B. K. Meyer, S. B. Orlinskii, J. Schmidt, and P. G. Baranov, Phys. Rev. Lett. **88**, 045504 (2002).
[46] S. F. Cox *et al.*, Phys. Rev. Lett. **86**, 2601 (2001).
[47] C. Kittle, *Introduction to Solid State Physics* (Wiley, New York, 1986).
[48] *Optical Properties of Solids*, edited by J. Tauc and F. Abèles (North-Holland, Amsterdam, 1971), p. 277.
[49] B. E. Sernelius, K.-F. Berggren, J. C. Jin, I. Hamberg, and C. G. Granquist, Phys. Rev. B **37**, 10244 (1988).
[50] N. Y. Garces, L. Wang, L. Bai, N. C. Giles, L. E. Halliburton, and G. Cantwell, Appl. Phys. Lett. **81**, 622 (2002).
[51] K. Vanheusden, C. H. Seager, W. L. Warren, D. R. Tallant, J. Caruso, M. J. Hampden-Smith, and T. T. Kodas, J. Lumin. **75**, 11 (1997).
[52] N. Ohashi, T. Ishigaki, N. Okada, T. Sekiguchi, I. Sakaguchi, and H. Haneda, Appl. Phys. Lett. **80**, 2869 (2002).
[53] S. Im, B. J. Jin, and S. Yi, J. Appl. Phys. **87**, 4558 (2000).
[54] V. Srikant and D. R. Clarke, J. Appl. Phys. **83**, 5447 (1998).
[55] M. M. M. Bilek, M. Chhowalla, and W. I. Milne, Appl. Phys. Lett. **71**, 1777 (1997).
[56] H. Kelly, A. Lepone, and A. Marquez, J. Appl. Phys. **89**, 1567 (2001).
[57] A. Lepone, H. Kelly, and A. Marquez, J. Appl. Phys. **90**, 3174 (2001).
[58] A. F. Kohan, G. Ceder, D. Morgan, and C. G. Van de Walle, Phys. Rev. B **61**, 15019 (2000).

Downloaded 07 Aug 2003 to 155.69.4.4. Redistribution subject to AIP license or copyright, see http://ojps.aip.org/japo/japcr.jsp